

# iDQC MR Imaging with Contrast of Off-resonance Rotating-frame Spin-Lattice Relaxation

B. Zheng<sup>1</sup>, Z. Chen<sup>1,2</sup>, S. D. Kennedy<sup>3</sup>, J. Zhong<sup>2</sup>

<sup>1</sup>Department of Physics and Research Center of Biomedical Engineering, Xiamen University, Xiamen, Fujian, China, People's Republic of, <sup>2</sup>Departments of Radiology and Biomedical Engineering, University of Rochester, Rochester, NY, United States, <sup>3</sup>Department of biophysics and biochemistry, University of Rochester, Rochester, NY, United States

## Introduction

A long-duration, low-power, and off-resonance spin-locking pulse was incorporated into the CRAZED sequence in order to measure the intermolecular double-quantum longitudinal relaxation time  $T_{1\rho,DQ}^{eff}$  in the tilted rotating frame. This modified CRAZED sequence was also appended to a standard fast spin-echo imaging sequence (shown in the bracket of Fig. (1)) to form images with  $T_{1\rho,DQ}^{eff}$ -weighted contrast.

## Methods

In Fig. 1, the low-power rf pulse  $(\omega_1)_y$  and frequency offset  $\Delta\omega$  constitute an effective spin-locking field along the  $z'$  axis of a tilted rotating frame, with an effective frequency  $\omega_e = \sqrt{(\omega_1)^2 + \Delta\omega^2}$  and a tilt angle  $\theta = \arctan(\omega_1/\Delta\omega)$  with respect to the normal Larmor rotating frame ( $\theta = \pi/2$  for an on-resonance spin-locking pulse without frequency offset) [1,2]. The magnetization aligned along the effective field  $\omega_e$  relaxes with a relaxation time constant during the locking period  $T_{SL}$ . For iDQCs, the final observable transverse magnetization becomes [3]

$$M_+^{DQ}(t_2, \theta) = \frac{1}{4} i \gamma \mu_0 t_2 \sin^2 \theta \sin \beta (1 - \cos \beta) M_0^2 e^{-T_{SL}/T_{1\rho,DQ}^{eff}} e^{-t_2/T_2}. \quad (1)$$

Here we define an off-resonance iDQC longitudinal relaxation in the tilted rotating frame,  $T_{1\rho,DQ}^{eff}$ . For the weak-collision limit,  $T_{1\rho,DQ}^{eff}$  can be written as [1],

$$\frac{1}{T_{1\rho,DQ}^{eff}} = \frac{K}{2} [\sin^4 \theta J_0(2\omega_e) + \sin^2 \theta \cos^2 \theta J_0(\omega_e) + aJ_1(\omega_0) + bJ_2(2\omega_0)], \quad (2)$$

where  $a$  and  $b$  are coefficients of spectral densities;  $K$  is a constant including information of local field fluctuation;  $J_0$ ,  $J_1$ , and  $J_2$  are corresponding spectral density functions, respectively [1]. Equation (2) shows that, in a system of slow-motion molecules (such as large macromolecules and biomolecules *in vivo*), the dominant term at low frequency is  $J_0(2\omega_e)$  and  $J_0(\omega_e)$ .

MRI studies were performed on a 600-MHz Varian Inova NMR spectrometer. A phantom was made from water-based agarose gels in two tubes of different internal diameters, with 2.5% (W/V) gel in the inner compartment and 1% (W/V) in the outer one. The measurement parameters were as follows: TR = 3 s, FOV = 6 mm × 6 mm, slice thickness = 0.5 mm, echo train length (ETL) = 4, and matrix size = 64 × 64.

A mice tail was placed in a standard 5-mm NMR tube and imaged in the sagittal plane. FOV = 10 mm × 5 mm, slice thickness = 0.3 mm, matrix size = 128 × 64, ETL = 4, TR = 5 s, and echo spacing = 7 ms. The correlation gradient with strength G of 128 mT/m and duration δ of 1 ms was applied along the z direction. A four-step phase-cycling scheme was used to remove residual conventional SQC signals.

## Results and discussion

Figure 2 shows the phantom images with contrast weighted by  $T_{1\rho,DQ}^{eff}$  or  $T_{2,DQ}$ . It shows that the decay of signal intensity of the  $T_{2,DQ}$ -weighted images is much faster than that of the  $T_{1\rho,DQ}^{eff}$ -weighted ones. With the decrease of tilt angle  $\theta$ , the relaxation time  $T_{1\rho,DQ}^{eff}$  tends to increase in the two regions of the phantom. Figure 3 shows a series of images of a mice tail with varying duration of the locking field. The corresponding relaxation times measured from the ROIs were summarized in Fig. 4. Figure 4(a) shows that, with the increase of effective spin-locking frequency  $\omega_e$ , the measured relaxation times  $T_{1\rho,DQ}^{eff}$  of both cartilage and muscle increase. Figure 4(b) shows that the decrease of the tilt angle significantly increases the value of relaxation time  $T_{1\rho,DQ}^{eff}$ , and the tilt angle alter the contrast between two types of tissues when a fixed  $\omega_e$  is used. Therefore, both the tilt angle  $\theta$  and the effective spin-locking frequency  $\omega_e$  can be used as controllable parameters to manipulate image contrast. The off-resonance spin-locking imaging technique reduces the absorption of rf energy and is potentially feasible for clinical applications.

## Acknowledgment

This work was supported by the NNSF of China under Grant 10234070, NCET and EYTP of Ministry of Education of China, and NIH under Grant NS41048.

## References

- [1] Jones GP. *Phys. Rev.*, 148, 332, 1966. [2] Zheng BW, et al. *Magn. Reson. Med.*, 53, 930, 2005. [3] Zhong JH, et al. *Magn. Reson. Med.*, 43, 335, 2000.

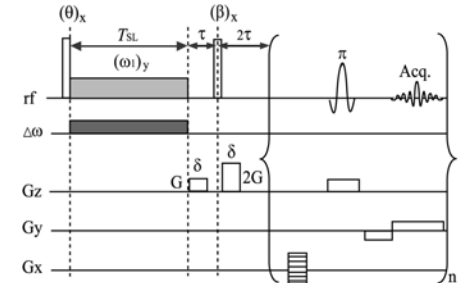


FIG. 1. Pulse sequence for forming iDQC images weighted by the off-resonance longitudinal relaxation in the tilted rotating frame.

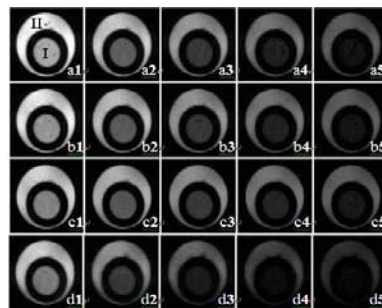


FIG. 2. Images of an agarose-gel phantom. (a1)-(a5) images acquired with the spin-locking duration  $T_{SL}$  of 10, 30, 50, 70, and 90 ms, respectively, and a tilt angle  $\theta=80^\circ$  and spin-locking frequency  $\omega_1=8.97$  kHz; (b1)-(b5) and (c1)-(c5) same as (a1)-(a5) with the tile angles  $\theta=70^\circ$  and  $\theta=60^\circ$ , respectively; (d1)-(d5) the  $T_{2,DQ}$ -weighting images acquired with the evolution time  $\tau$  of 10, 30, 50, 70, and 90 ms, respectively.

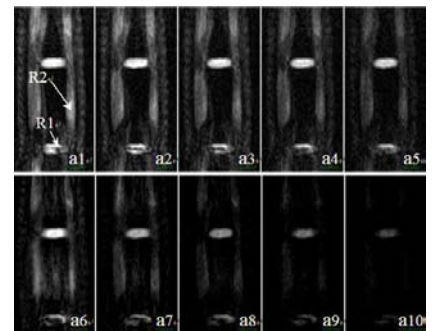


FIG. 3. Sagittal images of a mice tail sample. (a1)-(a5) the images for a tilt angle  $\theta = 70^\circ$  and an effective spin-locking frequency  $\omega_e = 8.71$  kHz with varied duration  $T_{SL}$  of 5, 10, 16, 24, 34 ms, respectively; (a6)-(a10) the  $T_{2,DQ}$ -weighting images with varied  $\tau$  of 5, 10, 16, 24, and 34 ms, respectively.

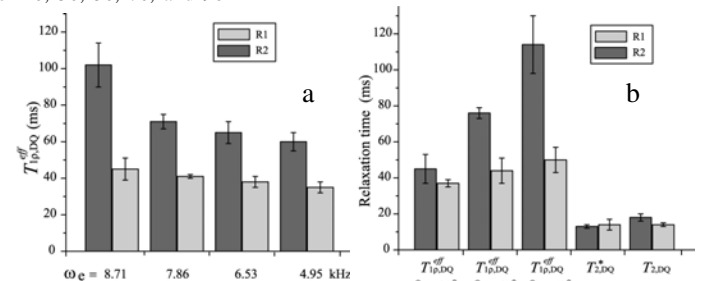


FIG. 4. (a) The relaxation times  $T_{1\rho,DQ}^{eff}$  measured in the ROIs from the images of the mice tail at a fixed tile angle of  $70^\circ$  and varied  $\omega_e$ . (b) The measured  $T_{1\rho,DQ}^{eff}$  at a fixed  $\omega_e$  and varied tile angles, plus the measured  $T_{2,DQ}^*$  and  $T_{2,DQ}$  values.